

Electronic structure of silver-deficient hexagonal AgB₂

I.R. Shein*, N.I. Medvedeva and A.L. Ivanovskii

Institute of Solid State Chemistry, Ural Branch of the Russian Academy of Sciences, 620219, Ekaterinburg, Russia

Electronic structure and cohesive properties of metastable hexagonal AgB₂ and silver-deficient borides Ag_{0.875}B₂ and Ag_{0.750}B₂ were investigated by means of the projected augmented wave method in the framework of the density functional theory (VASP package). We found that the density of states at the Fermi level for nonstoichiometric diborides is almost constant within a range of vacancy content up to 25%. The formation energy of metal vacancies in silver diboride is the least among all 4d metal diborides, i.e. for AgB₂ is possible to expect the wide homogeneity region.

* E-mail: shein@ihim.uran.ru

PACS numbers:

After the discovery of superconductivity with $T_c \sim 39$ K¹ in layered MgB₂, there have been a lot of theoretical searches for the potential superconductors with high T_c among other diborides MB₂ (M = Na, Be, Ca, noble and transition metals)^{2,3,4,5,6,7,8,9,10,11}, see also review¹². Among them the silver diboride (AgB₂) was predicted to be promising system having the larger density of B2p σ -like states near the Fermi level⁴ and electron-phonon coupling constant than MgB₂ and hence higher T_c ($\sim 60 \div 70$ K)^{7,8}.

However the attempts to synthesize AgB₂ lead to inconsistent results. For the first time the synthesis of AgB₂ phase (space group P6/mmm, lattice parameters $a = 3.00$ and $c = 3.24$ Å) has been declared thirty years ago¹³. Further the different experimental routes were used¹⁴ to obtain AgB₂ samples as a bulk and thin films; however all synthesized AgB₂ samples were unstable.

Quite recently the successful synthesis of silver boride thin films with nominal composition AgB₂ was performed by a pulsed laser deposition method¹⁵ and sharp superconducting transition was observed on the resistivity with the onset of superconductivity at 7.4 K and the zero resistance near 6.7 K. Thus the measurements¹⁵ confirmed the superconductivity in the silver boride system. However the observed T_c was significantly lower than the theoretically predicted value^{7,8} and comparable with T_c for some d metal diborides: ZrB₂ (5.5 K), TaB₂ (9.5 K) and NbB₂ (5.2K)¹².

This discrepancy may be caused by the inhomogeneous structure of the AgB₂ films, in particular by nonstoichiometry of samples. Recently was established^{16,17,18}, that some d metal diborides at nonequilibrium conditions may contain a significant amount of metal vacancies (for Nb_{1-x}B₂ and Ta_{1-x}B₂ up to $x \sim 0.48$). The band structure calculations¹⁹ showed that the metal vacancies are most likely to appear in diborides with rather weak M-B covalent bonding. It may be expected the presence of significant concentration of Ag vacancies in metastable AgB₂.

In this paper, we concentrate on the effects of Ag vacancies on the electronic and cohesive properties of silver

TABLE I: Lattice parameters a and c (Å), cell volume V_0 (Å³), bulk modulus B_0 (GPa), its pressure derivative B'_0 , intra- α_a and interlayer α_c (TPa⁻¹) linear compressibility for AgB₂: experiment and theory.

Parameters	Experiment		Theory ^a		
	see ¹³		see ⁷	see ²⁶	Our data
a	3.000	3.040 ^{25b}	2.980	3.000	3.024
c	3.024	3.180 ¹⁴	3.920	3.617	4.085
c/a	1.0800	-	1.3154	1.2051	1.3414
V_0	25.253	-	30.147	28.188	32.361
B_0	-	-	-	239	142
B'_0	-	-	-	3.20	4.00
α_a ^c	-	-	-	-0.93	-1.35
α_c	-	-	-	-2.10	-3.06

^aFLAPW⁷ and LCAO SCF Hartree-Fock²⁶ calculations

^bextrapolated from the Vegard relationship for Ag-doped MgB₂

^cThe isostatic pressure effect on the lattice constants generally expressed as: $a = a_0(1 + \alpha_a P)$ and $c = c_0(1 + \alpha_c P)$, where P is the pressure in GPa, α_a and α_c are axial compressibilities

diboride. For this purpose, the electronic structure of hexagonal AgB₂, as well as Ag-deficient Ag_{1-x}B₂ ($x = 0.875$ and 0.750) are investigated theoretically using the projected augmented wave (PAW) method in the framework of the density functional theory (the Vienna ab initio simulation package - VASP^{20,21,22,23}) with generalized gradient approximation (GGA) for exchange-correlation potential²⁴.

The silver diboride have the hexagonal crystal structure (space group P6/mmm) composed of layers of trigonal

prisms of Ag atoms in the center of boron atoms, which form the planar graphite-like networks. Both complete and nonstoichiometric AgB_2 phases were simulated by the 24-atoms supercell (Ag_8B_{16}). The removing of one silver atom ($\text{Ag}_7\text{V}^{\text{Ag}}\text{B}_{16}$, where V^{Ag} is the silver vacancy) describes the $\text{Ag}_{0.875}\text{B}_2$ composition. For the $\text{Ag}_{0.750}\text{B}_2$ composition (supercell $\text{Ag}_6\text{V}_2^{\text{Ag}}\text{B}_{16}$) some possible distributions of Ag vacancies are checked. For this purpose two vacancies (in cell) were located at the nearest positions in the Ag sheets, i.e. the alternation of complete and V^{Ag} -containing sheets along c-axis is described (case I). Secondly, two vacancies were placed in the neighbor sheets, and the "uniform" distribution of vacancies in a crystal was modeled (case II), Fig. 1. For all systems the structural parameters a and c have been optimized.

Let's discuss the data concerning an ideal AgB_2 phase. Table 1 shows the optimized lattice parameters of AgB_2 as well as the zero pressure bulk modulus B_0 and its pressure derivative ($B'_0 = dB_0/dP$) in comparison with some previous experimental and theoretical results. There is a significant difference between the contraction rates of intra- and inter-planar periodicity: the compressibility in AgB_2 is strongly anisotropic and the structure is more compressible in the z direction ($c=c_0(1-0.00360P)$) than in the xy plane ($a=a_0(1-0.00106P)$) (P in GPa). Thus, the interlayer linear compressibility exceeds the intralayer linear compressibility about 2.3 times.

The calculated heat of formation (ΔH , defined as a difference in the total energies of AgB_2 with reference to the E_{tot} of the constituent elements in their stable modifications: fcc-Ag and rhombohedral boron ($\alpha\text{-B}_{12}$)) has a small, but negative value (-0.98 eV/f.u.) testifying the possibility of AgB_2 synthesis. For comparison, ΔH for stable refractory 4d metal diborides ZrB_2 and NbB_2 were found to be -4.76 and -3.68 eV/f.u., respectively (FLMTO calculations¹⁹). The cohesive energy ($E_{\text{coh}} \sim 14.1$ eV/f.u.) is also minimal for AgB_2 in comparison with other 4d metal diborides: 23.4, 24.8 and 19.3 eV/f.u. for ZrB_2 , NbB_2 and YB_2 ¹⁹. The metastable nature of AgB_2 is determined by the very weak inter-layer Ag-B and intra-layer Ag-Ag interactions. The bonding picture may be examined using the difference electron densities ($\Delta\rho$), where neutral atomic charge ρ^{at} densities are subtracted from the crystalline density ρ^{cryst} , Fig.2. Negative $\Delta\rho$ around Ag and positive ones around boron indicate a charge transfer from Ag to B. The $\Delta\rho$ map shows a strongly covalent B-B bonding in the hexagonal boron sheets. On the contrary, the partial ionic type of the inter-plane Ag-B bonding occurs. The in-plane Ag-Ag bonds are insignificant: (i) the near-spherical symmetry of silver $\Delta\rho$ contours confirm the absence of Ag-Ag covalency; (ii) the ionic interaction between silver ions is repulsive and (iii) the Ag-Ag distance in diboride (3.004 Å) is about 4% higher than in fcc Ag (2.889 Å) i.e. the decrease in metallic-like bonding also occurs.

The electronic band structure of AgB_2 obtained in our calculations coincides with the previous results^{4,7}. The

B2p σ -like (in-plane) bands have a small dispersion along Γ -A-L in the BZ and form the hole Fermi surfaces⁴. The most attractive feature of AgB_2 is that the B2p σ -like bands are more flat than in MgB_2 , yielding the higher density of states at the Fermi level ($N(E_F)$). We found that $N(E_F) = 0.90$ states/eVcell, it is about 20% larger than in MgB_2 ($N(E_F) = 0.72$ states/eVcell). Calculated densities of states for AgB_2 , $\text{Ag}_{0.875}\text{B}_2$ and $\text{Ag}_{0.750}\text{B}_2$ are shown in Fig. 3. The occupied Ag 4d bands are located mainly in the region of $-5.8 \div -3.3$ eV. The upper part of conduction band is composed by comparable contributions of Ag 4d and antibonding B 2p states.

Let us consider the effect of silver vacancies on the structural, cohesion and electronic properties of AgB_2 . The introducing of V^{Ag} leads to the reduction of both lattice constants; however for $x = 0.125$ the c/a ratio decreases, whereas for $x = 0.250$ this parameter grows and it appears larger, than that for complete AgB_2 , Table 2. The inter-planar compression is more pronounced for the "uniform" V^{Ag} distribution (model II).

The energies of vacancy formation (E_{vf}) as well as E_{coh} and ΔH for $\text{Ag}_{1-x}\text{B}_2$ phases are summarized in Table 2. These parameters are calculated as:

$$E_{\text{vf}} = E_{\text{tot}}^{\text{AgB}_2} - E_{\text{tot}}^{\text{Ag}_{1-x}\text{B}_2} - xE_{\text{tot}}^{\text{Ag}}, \quad (1)$$

$$E_{\text{coh}}^{\text{Ag}_{1-x}\text{B}_2} = E_{\text{tot}}^{\text{Ag}_{1-x}\text{B}_2} - [(1-x)E_{\text{at}}^{\text{Ag}} + 2E_{\text{at}}^{\text{B}}], \quad (2)$$

$$\Delta H^{\text{Ag}_{1-x}\text{B}_2} = E_{\text{tot}}^{\text{Ag}_{1-x}\text{B}_2} - [(1-x)E_{\text{tot}}^{\text{Ag}} + 2E_{\text{tot}}^{\text{B}}], \quad (3)$$

where $E_{\text{at}}^{\text{Ag}}$, E_{at}^{B} are the total energies of free silver and boron atoms, $E_{\text{tot}}^{\text{Ag}}$, $E_{\text{tot}}^{\text{B}}$ are the total energies of fcc Ag metal and α -boron; and $E_{\text{tot}}^{\text{AgB}_2}$, $E_{\text{tot}}^{\text{Ag}_{1-x}\text{B}_2}$ are the total energies (per formula units) of AgB_2 and $\text{Ag}_{1-x}\text{B}_2$, respectively.

The calculated vacancy formation energy (0.34 eV) is essentially less than for $\text{Nb}_{1-x}\text{B}_2$ ($E_{\text{vf}} \sim 1.1$ eV¹⁹) where the metal vacancies were found experimentally^{16,17,18}. Hence, their presence is very probably in AgB_2 and the stoichiometry of AgB_2 based materials will be very sensitive to the synthesis conditions.

The redistribution of the charge states near V^{Ag} is demonstrated in Fig. 2. As is seen, in the Ag-deficient boride the B-B bonds remain almost undistorted. No new bonds going through the vacancy are formed. The difference map shows a weak density accumulation along the $\text{B} \rightarrow \text{V}^{\text{Ag}}$ direction, however the absence of the electron localization on the vacancy clearly follows from $\Delta\rho$ contour distribution in the planar (100) silver sheet, i.e. the charge states of silver vacancies are close to neutral. In the vicinity of vacancy only insignificant deformation

TABLE II: Lattice parameters (\AA), cohesive energies (E_{coh}), heat of formation (ΔH) and vacancy formation energies (E_{vf}) in eV/f.u. for complete and silver-deficient Ag borides.

Diborides	a	c	c/a	E_{coh}	ΔH	E_{vf}
AgB ₂	3.024	4.085	1.3414	14.06	-0.98	-
Ag _{0.875} B ₂	3.008	4.020	1.3364	13.71	-0.64	0.34
Ag _{0.75} B ₂ (I)	2.942	3.960	1.3460	13.32	-0.26	0.71
Ag _{0.75} B ₂ (II)	2.950	3.950	1.3551	13.35	-0.27	0.70

of $\Delta\rho$ contours appears along the direction $\text{Ag} \rightarrow \text{V}^{Ag}$. Figure 3 shows the changes in the DOS near the Fermi level with Ag-vacancies concentration in $\text{Ag}_{1-x}\text{B}_2$. The Fermi level slightly shifts towards the low energies with

increasing x , while the dependence of $N(E_F)$ is not sensitive to vacancy concentration. The $N(E_F)$ values for $\text{Ag}_{0.875}\text{B}_2$ and $\text{Ag}_{0.750}\text{B}_2$ are 0.88 and 0.92 states/eVcell, respectively.

In summary, we presented the results of band structure calculations for silver-deficient AgB_2 performed by the VASP method. It was established that vacancies are likely to appear in AgB_2 : the energy of metal vacancies formation in silver diboride is the least among all 4d metal diborides. Thus, the nonstoichiometry on Ag-sublattice will be easily achievable, i.e. for AgB_2 it is possible to expect the wide homogeneity region. Our analysis indicates that metal vacancies in AgB_2 do not lead to essential reduction of $N(E_F)$ which seems to be critical in depressing of the superconductivity in this system.

Acknowledgment.

This work was supported by the RFBR, grants 02-03-32971 and 04-03-32082.

-
- ¹ J. Nagamatsu, N.Nakagawa, T.Muranaka, Y.Zenitani, and J. Akimitsu, Nature (London), **410**, 63 (2001).
 - ² P. Vajeeston, P. Ravindran, C. Ravi, and R. Asokamani, Phys. Rev., **B63**, 5115 (2001).
 - ³ S. Suzuki, S. Higai, and K. Nakao, J. Phys. Soc. Jpn., **70**, 1206 (2001).
 - ⁴ I.R. Shein, N.I. Medvedeva, and A.L. Ivanovskii, Phys. Solid State **43**, 2213 (2001).
 - ⁵ N.I. Medvedeva, A.L. Ivanovskii, J.E. Medvedeva, and A.J. Freeman, Phys. Rev., **B64**, R020502 (2001).
 - ⁶ M.J. Mehl, D. A. Papaconstantopoulos, and S. Singh, Phys. Rev., **B64**, 140509 (2001).
 - ⁷ S.K. Kwon, S.J. Youn, K.S. Kim, and B.I. Min, Cond-matter/0106483 (2001).
 - ⁸ F. Yang, R.S. Han, N.H. Tong and W. Guo, Chinese Phys. Lett., **19**, 1336 (2002).
 - ⁹ T. Oguchi, J. Phys. Soc. Jpn., **71**, 1495 (2002).
 - ¹⁰ I.R. Shein, N.I. Medvedeva, and A.L. Ivanovski, Phys. Solid State **44**, 1833 (2002).
 - ¹¹ G. Profeta, A. Continenza, F. Bernardini, S. Massidda, Phys. Rev., **B65**, art no. 054502 (2002).
 - ¹² A.L. Ivanovskii, Phys. Solid State,**45**, 1829 (2003).
 - ¹³ V.N. Gurin and M.M. Korsukova, in Boron and Refractory Borides edited by V.I. Matkovich (Springer-Verlag Berlin Heidelbergm New York 1977) p. 301.
 - ¹⁴ M. Sinder and J. Pelleg, cond-mat/0212632 (2002).
 - ¹⁵ R. Tomita, H. Koga, T. Uchiyama and I. Iguchi, J. Phys. Soc. Japan, **73**, 2639 (2004).
 - ¹⁶ A. Yamamoto, C. Takao, T. Masui, M. Izumi and S. Tajima, Physica C, **383**, 197 (2002).
 - ¹⁷ H. Takeya, A. Matsumoto, K. Hirata, Y.S. Sung and K. Togano, Physica C, **412-414**, 111 (2004).
 - ¹⁸ H. Takeya, K. Togano, Y. S. Sung, T. Mochiku and K. Hirata, Physica C, **408-410**, 144 (2004).
 - ¹⁹ I. R. Shein, N. I. Medvedeva, and A. L. Ivanovskii, Phys. Solid State, **45**, 1617(2003).
 - ²⁰ G. Kresse, J. Hafner, Phys. Rev., **B47**, 558 (1993).
 - ²¹ G. Kresse, J. Furthmuller, Comput. Mat. Sci., **6**, 15 (1996).
 - ²² G. Kresse, J. Furthmuller, Phys. Rev., **B54**, 11169 (1996).
 - ²³ G. Kresse, J. Joubert, Phys. Rev., **B59**, 1758 (1999).
 - ²⁴ J.P. Perdew, K. Burke, M. Ernzerhof, Phys. Rev. Lett., **77**, (1996) 3865.
 - ²⁵ C.H. Cheng, Y. Zhao, X.T. Zhu, J. Nowotny, C.C. Sorrell, T. Finlayson and H. Zhang, Physica C, **386**, 588 (2003).
 - ²⁶ F. Parvin, A.K.M.A. Islam, F.N. Islam, A.F.M.A. Wahed and M.E. Haque, Physica C, **390**, 16 (2003).

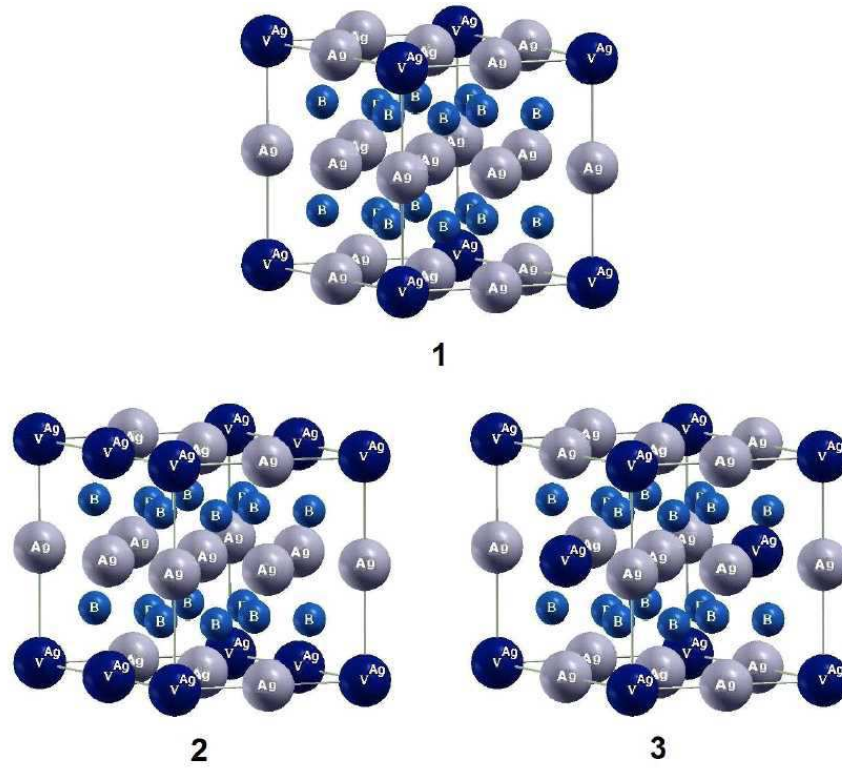


FIG. 1: Fig. 1. Structural models for silver-deficient $\text{Ag}_{1-x}\text{B}_2$: 1 - $\text{Ag}_{0.875}\text{B}_2$ and 2,3 - $\text{Ag}_{0.750}\text{B}_2$. The possible distribution of Ag vacancies (V^{Ag}) are presented: 2 - the alternation of complete and V^{Ag} -containing sheets (along z-axis, model I) and 3 - the "uniform" V^{Ag} distribution (model II), respectively.

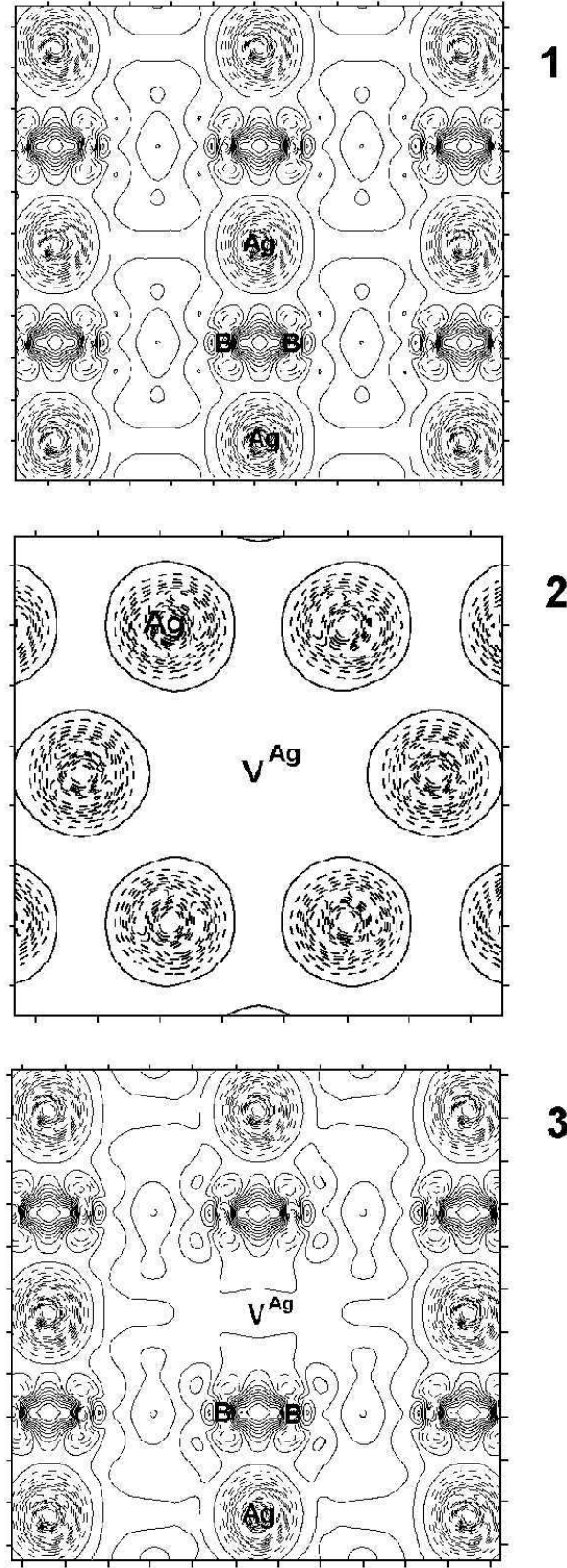


FIG. 2: Fig. 2. Inter-plane charge-density difference ($\Delta\rho$) maps for AgB_2 (1), $\text{Ag}_{0.875}\text{B}_2$ (3) and $\Delta\rho$ map in (100) silver sheet of $\text{Ag}_{0.875}\text{B}_2$. In the $\Delta\rho$ plots, solid and dashed lines indicate an increase and a decrease of the electron density $\Delta\rho^{\text{AgB}_2}$ relative to the atomic (ρ^{Ag} , ρ^{B}) superposition, respectively.

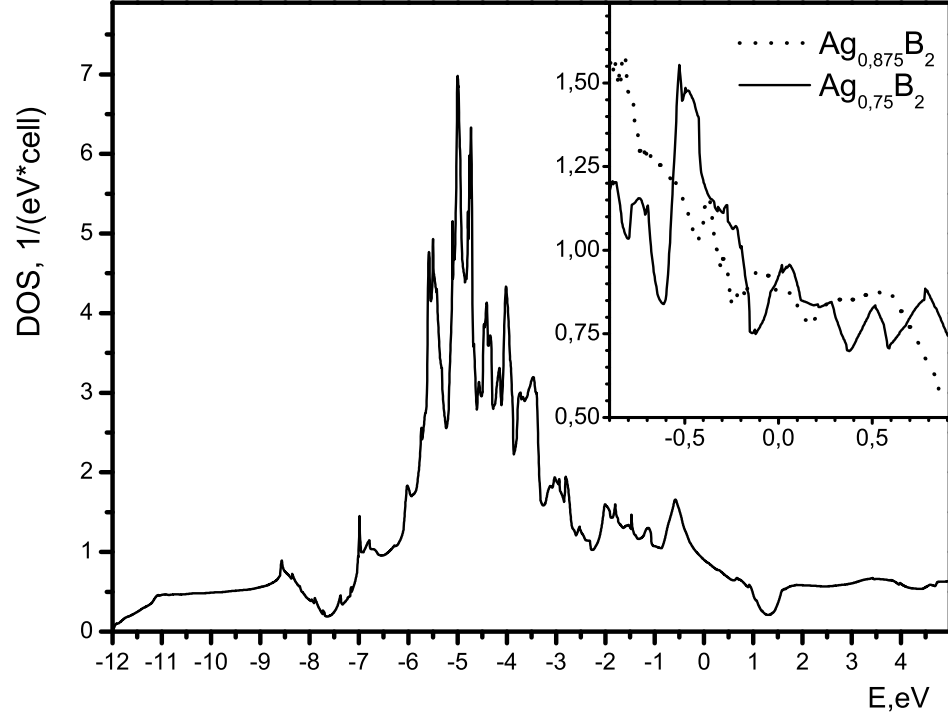


FIG. 3: Density of states for AgB_2 . *Inset* shows near-Fermi DOSs for $\text{Ag}_{0.875}\text{B}_2$ and $\text{Ag}_{0.75}\text{B}_2$. $E_F = 0$ eV.